



(RESEARCH ARTICLE)



Petrographic, mineralogical and microstructural studies in the mafic dyke occurred in the area of Mettur, Salem District, Tamil Nadu, India

Hari Prasad S., Senthil Kumar G.R.* and Faisal Abass Padder

Department of Earth Sciences, Annamalai University, Annamalainagar – 608 002, Tamil Nadu,, India.

GSC Advanced Research and Reviews, 2023, 14(03), 241–253

Publication history: Received on 09 February 2023; revised on 18 March 2023; accepted on 21 March 2023

Article DOI: <https://doi.org/10.30574/gscarr.2023.14.3.0088>

Abstract

A mafic dyke is a mass of rock generated in either sedimentary or igneous terrain and intrudes in pre-existing cracks. It was common to see many enormous dyke swarms in the southern granulitic landscape made up of archean rocks. Dykes tend to be younger than the surrounding rock body. Generally, mafic dolerite dyke has an ophitic texture and is medium to fine grained. In the study area country rock and dolerite dyke rocks petrographical microscope, XRD, and FE-SEM techniques were analysed. Plagioclase feldspar, augite, biotite, hornblende, and quartz minerals presented in the study area rocks. Alternating wedges, augite/labradorite grain boundaries are shown in the microstructure as a white rectangle. Two augite wedges were observed with rounded ends. The mineral percentage of quartz is rich in dolerite rock because of its intergrowth texture and low cooling temperature and pressure. So, the magma crystallized rapidly on the surface thus, the crystallizing temperature of the quartz is low. Thus, the rock mineral shows a high percentage of quartz. The rock is quartz-dolerite.

Keywords: Dyke; Petrography; Mineralogy; Microstructure; Quartz-Dolerite.

1. Introduction

Many of the Archaean gneissic terrains contain early Proterozoic dyke swarms as a common unit. The widespread occurrences is that partial melting in the mantle produced mafic dykes. However, little or microscale differences in various mafic dykes and other mantle-derived rocks, such as mantle xenoliths, have shown that the composition of mantle-derived rocks can differ greatly from the source. In general, there are two possible causes for variations in the composition of mafic rocks: first, variations in the source mantle; and second, variations in the processes of magma generation, such as the degree of partial melting or variations in the magmatic processes, such as fractional crystallisation and crustal assimilation. Typically, mafic dykes are connected to the extension of the continental lithosphere [1, 2, 3, 4] and their parent magmas came from sources in the deep mantle, opening a window to study the nature of the deep mantle and the development of the lithosphere [5]. The primary pathway by which mantle melts are delivered to the crustal levels is through the mafic dykes. These are important features, and in some cases, the sole significant Proterozoic geologic event that affected the Archaean cratons [6]. Although a few intrude Paleozoic sedimentary strata of the valley and ridge province, the majority of dykes are found in the Piedmont province. Individual dykes can be up to 100 km long, and local swarms can be up to 225 km long [7]. Although 300 m ± thick dykes exist [8], the majority are less than 30 m wide [9, 10]. Dykes occur in a wide variety of geological and tectonics settings and their detailed study through space and time is imperative for understanding several geological events. Dykes are believed to be an integral part of continental rifting and when they occur as spatially extensive swarms of adequate size can be of immense utility in continental reconstructions. This also helps to identify large igneous provinces (LIPs) [11]. Dykes are particularly important for serving as conduits for the transfer of voluminous magma from the mantle to the upper crust and thereby constitute a common expression of crustal extension. It is also well acknowledged that the continental flood basalts and major dyke swarms have their origin related in some way to the up-rise of hot mantle plumes which may

* Corresponding author: G. R. Senthil Kumar 0000-0002-8647-1959

lead to rifting and eventual continental break-up [12]. According to [13], dykes appear to have been formed by upwelling magma which mainly followed joints and cross faults. Most dykes are fairly straight, continuous, and parallel except where abundant longitudinal faults occur. The dip of most dykes is nearly vertical, but several have been observed to dip as low as 25°.

1.1. Geological setting of the study area

The study area is located near to the Yellikkaradu Village of Mettur Taluk of Salem District, Tamil Nadu, South India. The study area is located at a distance of 48 km towards the northwest of Salem, which is the headquarter of Salem District. The study area is marked in the Survey of India toposheet number 58E/9, 10, 13 & 14 with the coordinates 77°46'41" E and 11°46'23" N. The mafic dyke occurs on the eastern slope of the steep hill. The general trend of the dyke is N 50° to 60° W to S 50°- 60° E and dipping vertically. The study area dyke runs for several kms. However, for this study, we have taken about 800 m length of dyke body, the reason is that only a certain part of the area is approachable and convenient for collecting samples and preparing maps. The area receives moderate rainfall (40 cm per annum) and the rainy period is mainly due to the NE monsoon from October to December every year. The summer is hot with a maximum temperature of up to 36°C. The geological map of the study area is shown in Fig.1.

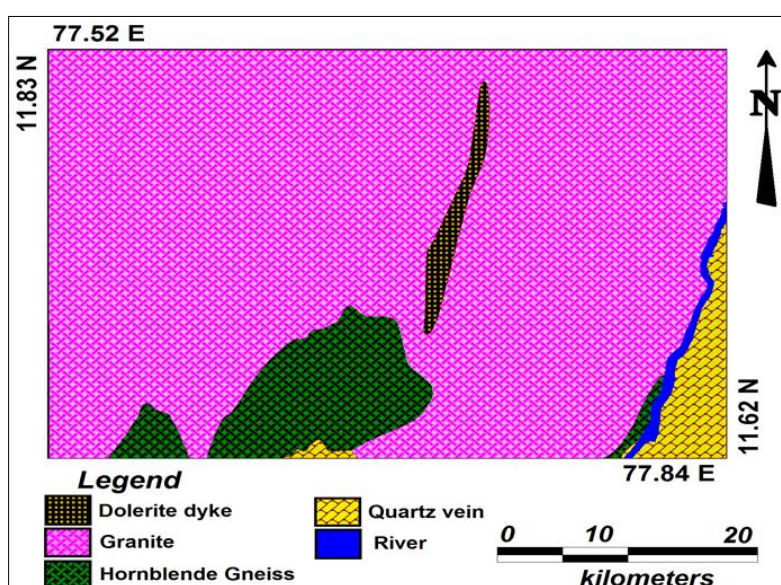


Figure 1 Geological map of the study area

2. Material and methods

2.1. Sample collection

Systematic fieldwork has been carried out to investigate the dolerite dyke of the study area. During the fieldwork ten representative specimens, including the dyke rock and country rock were collected. Generally, dyke is a uniform and homogenous body. So, in this study, two dyke samples and one country rock sample were taken for the analytical studies. The samples underwent for petrographical, X-ray diffraction and SEM analysis studies.

2.2. Sample preparation

2.2.1. Thin section preparation

The collected representative specimens were taken to the laboratory for preparation of thin sections. The thin sections were prepared by standard procedures, thin sections were made by the Department of Earth Sciences, Pondicherry University, Puducherry.

2.2.2. Powder samples for mineralogical analysis

The dried rock samples were crushed and pulverized into fine powder with the help of iron mortar. The powder samples were pouched, separated and sent for XRD analysis in order to understand mineralogical measurements. The XRD analysis performed at Department of Chemistry, Annamalai University.

2.2.3. Specimens for microstructure analysis

Samples were washed and dried at room temperature, and then the samples were cut and polished in the rock cutting and grinding lab, Department of Earth Sciences, Annamalai University. The polished specimens were coated for secondary imaging for microstructural investigations in the Central Sophisticated Instrumentation Lab (CSIL), Annamalai University.

2.3. Analytical method

2.3.1. Petrography

The microscopic investigations of thin sections were carried out at the Department of Geology, Periyar University, using a LEICA DM 2700P petrographic microscope. The minerals were investigated in plane polarised light (PPL) and crossed polarised light (XPL). The petrographical microscope was used to conduct in-depth textural and mineralogical examinations.

2.3.2. Mineralogy

The mineralogical characteristics of the dolerite and charnockite samples were determined using ARLEQUINOX 1000 X-RAY Diffractometer.

2.3.3. Microstructure

To examine the microstructures of the rocks, the dolerite and charnockite rock specimens are subjected to a field emission scanning electron microscope. It was carried out at Annamalai University's Central Sophisticated Instrumentation Lab. A Scanning Electron Microscope Eds Zeiss-Sigma 300fesem with the edax specification was used for the analysis.

3. Results and discussion

3.1. Dolerite (S1)

The important minerals, including augite, plagioclase feldspar, and opaque minerals, are depicted in dolerite (S1) the photomicrographs shown in Figure 2. In the sample dolerite (S1), biotite exhibits brownish colour and pleochroism display observed. The dykes generally have a sub-ophitic texture. True ophitic texture typically appears in the centre of dykes that are greater than 25 feet thick [14]. The grains show a subhedral shape and sub-ophitic texture. The effects of secondary alteration are shown by the presence of biotite, sericite, chlorite, serpentine, iddingsite and magnetite in concentrations up to 5% [15]. The edges of augite are altered to hornblende. The quartz and feldspar show intergrowth (granophyric) texture. The groundmass minerals show that the pyroxene began to crystallize before plagioclase. The specimen shows inter-mineral fracture under the microscope.

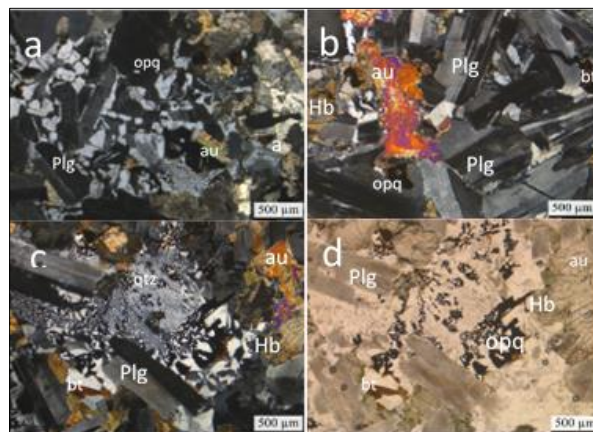


Figure 2 Photomicrographs: (a) thin section of dolerite with the presence of plagioclase feldspar (Plg), augite (aug) and opaque minerals. (b) thin section of dolerite with the presence of augite (aug), plagioclase feldspar (plg), hornblende (hb), biotite (bt) and opaque minerals. (c) thin section of dolerite with the presence of quartz (qtz), biotite (bt), augite (au), plagioclase feldspar (plg), and (d) plagioclase feldspar (plg), biotite (bt), augite (au), hornblende (hb) and opaque minerals.

3.2. Dolerite (S2)

The Figure 3, exhibits the photomicrographs of dolerite (S2). The essential minerals observed are plagioclase feldspar, augite, and opaque minerals. Biotite shows brownish colour, pleochroism and interference colour present in the sample. Augite shows violet, blue, and yellow as interference colours. The inclusions in the plagioclase are iron oxides mainly magnetite. The opaques consist of magnetite and sulphides (pyrite/pyrrhotite) in order of abundance. The laths of plagioclase show polysynthetic twinning and a cloudy appearance. The augite shows contact twinning, basal cleavage and edges altered to hornblende. Plagioclase edges show few sericite alterations. In this section, skeletal opaque intergrowth with granophyric texture observed.

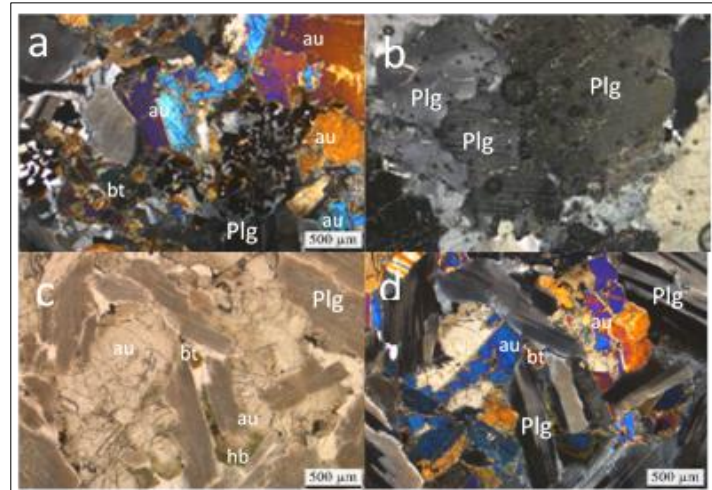


Figure 3 Photomicrographs of dolerite (S2) showing (a) thin section of dolerite with the presence of plagioclase feldspar (Plg), biotite (bt), augite (aug) and opaque minerals. (b) thin section of dolerite with the presence of plagioclase feldspar (plg). Photomicrographs under polariser showing (c) plagioclase feldspar (plg), biotite (bt), augite (au), and hornblende (hb) and (d) thin section of dolerite with the presence of biotite (bt), augite (au) and plagioclase feldspar (plg).

3.3. Charnockite (S3)

The photomicrographs (Fig. 4) show plagioclase and microcline quartz, biotite and hypersthene and opaque minerals. The grain size is medium to coarse and inequigranular. Sericite is the alteration product of plagioclase and quartz. Zircon present shows parallel extinction. The quartz and k-feldspar show intergrowth myrmekitic texture also observed.

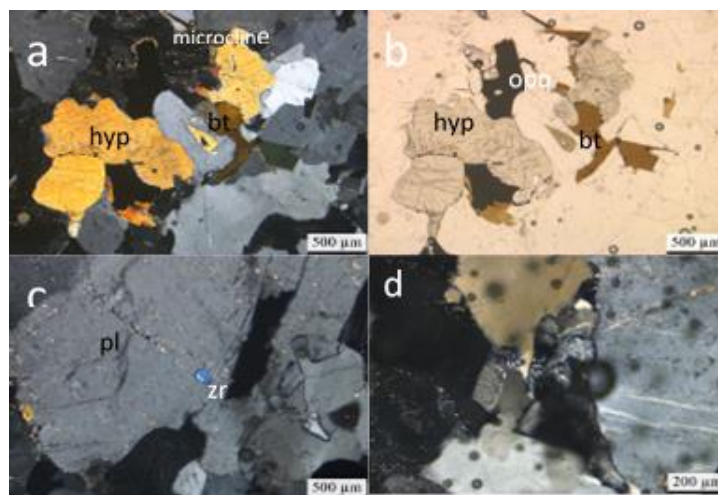


Figure 4 Photomicrographs under analyser showing (a) microcline, biotite (bt) and hypersthene (hyp). (b) plagioclase feldspar (plg), biotite (bt), hypersthene (hyp) and opaque minerals. (c) showing plagioclase feldspar (plg) and zircon (zr) and (d) showing intergrowth texture of quartz and microcline.

3.4. Mineralogy

3.4.1. Dolerite

The X-ray diffraction has shown to be one of the best tools for the identification and quantification of minerals present rock in soil [16]. Mineral compositions reveal that the complex petrogenetic evolutions which usually characterize dolerite dykes of continental setting [17, 18]. The mineral composition of the dolerite is composed of quartz, augite and plagioclase feldspar. Among the 51 XRD peaks 3 phases were identified, 23 peaks represent quartz mineral, 20 peaks report augite and the remaining 8 peaks reported plagioclase feldspar. The XRD pattern of dolerite is shown in Figure 5.

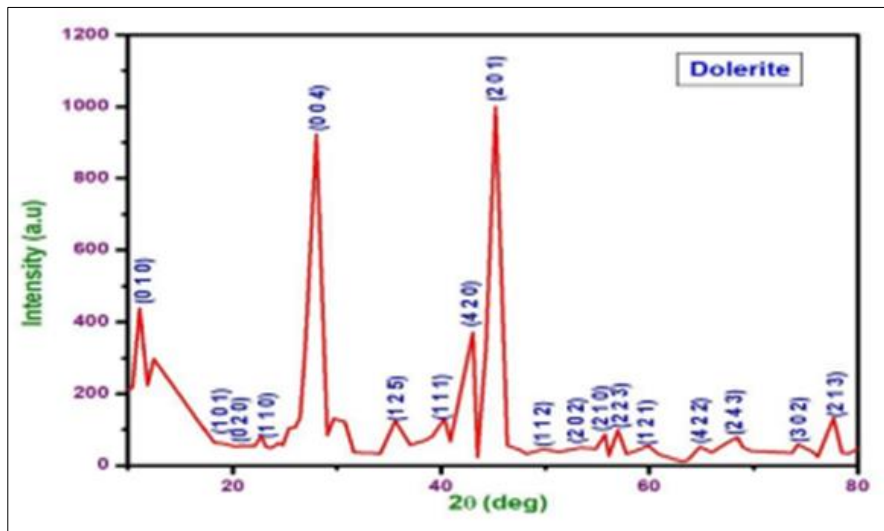


Figure 5 The XRD pattern of dolerite rock sample.

All the observed characteristic peaks (planes) are tabulated. From this, all the major and minor peaks are well matched with the dolerite mineral composition of JCPDSNo: 89-0572, and 88-2376. This indicates that the sample is in the form of dolerite. From this figure, the intensity of quartz planes is high compared with other minerals. It clearly shows, the presence of a large proposition of quartz in dolerite mineral (Ref. Table1). Some low-intensity peaks represent the minerals in trace levels in dolerite. Dolerite is composed of two essential and several accessory minerals. The essential minerals are plagioclase feldspar and pyroxene, which together constitute between about 60% and 80% of the total rock composition. The accessory minerals are quartz, orthoclase, chlorite and magnetite. Quartz, orthoclase and chlorite may comprise 20% to 40% of the rock while the magnetite composition may be consist 2% to 3%.

Table 1 XRD peak value details of dolerite rock

| 2 theta S [°] | d [Å] | I/10 (peak height) | Counts (peak area) | FWHM | Hkl value | Size (nm) | Phase Name | JCPDS File No. |
|---------------|--------|--------------------|--------------------|--------|-----------|-----------|------------|----------------|
| 11.09 | 7.9695 | 437.26 | 26.86 | 0.2411 | 0 1 0 | 34.618 | Quartz | 89-0572 |
| 12.48 | 7.0870 | 297.42 | 28.99 | 0.3827 | 1 1 0 | 21.78196 | Augite | 88-2376 |
| 18.18 | 4.8767 | 63.75 | 8.64 | 0.5321 | 1 0 1 | 15.5616 | Quartz | 89-0572 |
| 19.02 | 4.6622 | 61.41 | 7.69 | 0.4919 | 0 2 0 | 16.81316 | Augite | 88-2376 |
| 20.17 | 4.3999 | 53.83 | 6.95 | 0.5066 | 1 0 0 | 16.29702 | Quartz | 89-0572 |
| 22.92 | 4.2431 | 54.88 | 6.28 | 0.4494 | 1 1 0 | 18.28763 | Quartz | 89-0572 |
| 23.69 | 3.7524 | 48.10 | 5.53 | 0.4515 | 1 1 1 | 18.17736 | Augite | 88-2376 |
| 24.41 | 3.6428 | 62.84 | 5.42 | 0.3384 | 1 1 1 | 24.22016 | Augite | 88-2376 |

| | | | | | | | | |
|-------|--------|---------|-------|--------|-------|----------|-------------------------|---------|
| 25.38 | 3.5065 | 103.87 | 7.32 | 0.2765 | 1 3 2 | 29.58699 | Plagioclase feldspar | 20-0572 |
| 25.95 | 3.4304 | 106.27 | 8.05 | 0.2974 | 2 2 2 | 27.47659 | Plagioclase feldspar | 20-0572 |
| 26.46 | 3.3652 | 133.64 | 10.19 | 0.2994 | 1 1 4 | 27.26479 | Plagioclase feldspar | 20-0572 |
| 26.98 | 3.3024 | 331.07 | 25.52 | 0.3026 | 0 1 1 | 26.9474 | Quartz | 89-0572 |
| 28.03 | 3.1805 | 922.27 | 74.93 | 0.3189 | 0 0 4 | 25.51276 | Plagioclase feldspar | 20-0572 |
| 29.69 | 3.0066 | 131.22 | 9.39 | 0.2810 | 2 2 1 | 28.84607 | Augite | 88-2376 |
| 30.77 | 2.9030 | 120.95 | 12.96 | 0.4208 | 0 2 2 | 19.21373 | Plagioclase feldspar | 20-0572 |
| 31.65 | 2.8248 | 36.32 | 5.17 | 0.5590 | 1 3 2 | 14.43259 | Plagioclase feldspar | 20-0572 |
| 35.57 | 2.5220 | 123.75 | 10.46 | 0.3319 | 1 2 5 | 24.0581 | Plagioclase feldspar | 20-0572 |
| 37.04 | 2.4248 | 56.75 | 6.40 | 0.4427 | 1 3 1 | 17.96108 | Augite | 88-2376 |
| 38.40 | 2.3422 | 68.84 | 6.19 | 0.3532 | 1 0 2 | 22.42129 | Quartz | 89-0572 |
| 39.15 | 2.2989 | 80.45 | 7.88 | 0.3844 | 3 3 1 | 20.55406 | Plagioclase feldspar | 20-0572 |
| 40.30 | 2.2361 | 130.76 | 11.09 | 0.3329 | 1 1 1 | 23.6479 | Quartz | 89-0572 |
| 40.90 | 2.2046 | 67.74 | 6.94 | 0.4020 | 2 0 0 | 19.54516 | Quartz | 89-0572 |
| 43.04 | 2.0998 | 370.24 | 29.97 | 0.3177 | 4 2 1 | 24.55484 | Augite | 88-2376 |
| 43.49 | 2.0790 | 23.74 | 1.03 | 0.1697 | 4 2 0 | 45.89825 | Augite | 88-2376 |
| 45.24 | 2.0026 | 1000.00 | 61.42 | 0.2411 | 2 0 1 | 32.10527 | Quartz | 89-0572 |
| 46.36 | 1.9570 | 55.91 | 15.45 | 1.0850 | 1 3 2 | 7.104783 | Augite | 88-2376 |
| 49.85 | 1.8277 | 46.03 | 16.96 | 1.4467 | 1 1 2 | 5.256516 | Quartz | 89-0572 |
| 51.36 | 1.7775 | 37.38 | 13.20 | 1.3864 | 0 0 3 | 5.451078 | Quartz | 89-0572 |
| 53.38 | 1.7149 | 49.31 | 16.66 | 1.3262 | 2 0 2 | 5.649334 | Quartz | 89-0572 |
| 54.89 | 1.6714 | 46.75 | 9.33 | 0.7836 | 0 2 2 | 9.497021 | Quartz | 89-0572 |
| 55.73 | 1.6480 | 86.40 | 9.29 | 0.4220 | 2 1 0 | 17.56714 | Quartz | 89-0572 |
| 56.12 | 1.6375 | 26.57 | 9.38 | 1.3864 | 2 2 3 | 5.337531 | Augite | 88-2376 |
| 57.00 | 1.6144 | 98.21 | 16.59 | 0.6631 | 4 4 0 | 11.11362 | Augite | 88-2376 |
| 57.81 | 1.5936 | 32.73 | 3.52 | 0.4220 | 4 4 0 | 17.39568 | Augite | 88-2376 |
| 58.53 | 1.5756 | 38.48 | 7.68 | 0.7836 | 2 1 1 | 9.335583 | Quartz | 89-0572 |
| 59.95 | 1.5417 | 55.08 | 3.99 | 0.2841 | 1 2 1 | 25.56848 | Quartz | 89-0572 |
| 60.94 | 1.5189 | 30.43 | 6.48 | 0.8364 | 1 1 3 | 8.641246 | Quartz | 89-0572 |
| 63.21 | 1.4699 | 9.76 | 0.99 | 0.3992 | 3 3 3 | 17.89051 | Augite | 88-2376 |
| 63.72 | 1.4593 | 15.76 | 6.08 | 1.5133 | 3 0 0 | 4.706444 | Quartz | 89-0572 |

| | | | | | | | | |
|-------|--------|--------|-------|--------|-------|----------|--------|---------|
| 64.92 | 1.4351 | 51.88 | 10.72 | 0.8109 | 4 2 2 | 8.725514 | Augite | 88-2376 |
| 66.04 | 1.4136 | 35.73 | 3.90 | 0.4288 | 2 0 3 | 16.39737 | Augite | 88-2376 |
| 68.45 | 1.3695 | 77.66 | 5.98 | 0.3023 | 2 4 3 | 22.93596 | Augite | 88-2376 |
| 68.93 | 1.3611 | 51.24 | 2.64 | 0.2026 | 7 1 1 | 34.125 | Augite | 88-2376 |
| 73.66 | 1.2849 | 34.25 | 1.21 | 0.1391 | 3 0 2 | 48.25315 | Quartz | 89-0572 |
| 74.24 | 1.2764 | 57.84 | 2.88 | 0.1958 | 0 6 2 | 34.14956 | Augite | 88-2376 |
| 75.68 | 1.2556 | 37.30 | 3.19 | 0.3353 | 2 0 0 | 19.75057 | Quartz | 89-0572 |
| 76.17 | 1.2488 | 24.01 | 1.17 | 0.1919 | 55 2 | 34.39451 | Augite | 88-2376 |
| 77.67 | 1.2283 | 131.81 | 9.22 | 0.2747 | 2 1 3 | 23.7788 | Quartz | 89-0572 |
| 78.43 | 1.2184 | 34.25 | 5.22 | 0.5978 | 1 1 4 | 10.86821 | Quartz | 89-0572 |
| 79.12 | 1.2095 | 34.16 | 2.57 | 0.2957 | 1 7 1 | 21.86329 | Augite | 88-2376 |
| 80.26 | 1.1951 | 50.04 | 9.05 | 0.7101 | 3 1 1 | 9.029046 | Quartz | 89-0572 |

3.4.2. Charnockite

The XRD pattern of the charnockite is given in Figure 6, and the mineral composition is shown in Table 2. Based on the details, charnockite sample consists 71 peaks, among the peaks, 28 peaks reported for microcline, the remaining 43 peaks were shared with olivine (18 peaks), hornblende (15 peaks), biotite (7 peaks) and hypersthene (3 peaks) respectively.

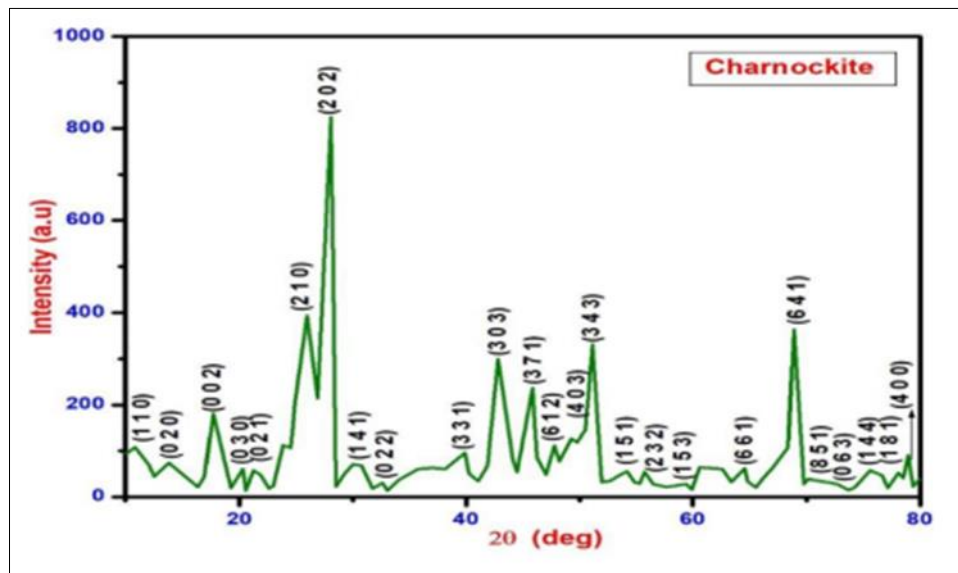


Figure 6 The XRD pattern of charnockite rock sample.

All the observed characteristic peaks (planes) are tabulated. From the table, all the major and minor peaks are well matched with the charnockite mineral composition of JCPDS No: 87-1792, and 85-1682. This indicates that the sample is in the form of charnockite. The pattern indicates that the intensity of the microcline plane is high compared with other minerals. It clearly shows the presence of large proportions of microcline in charnockite rock. Some low-intensity peaks represent the minerals in trace levels in charnockite. The mineral composition of charnockite is composed of microcline, hornblende, olivine, biotite and hypersthene. Microcline is rich in charnockite may be due to the rich composition of K which is rich in the magma during crystallization. Because microcline is a type of potash feldspar.

Table 2 XRD peak value details of charnockite rock

| 2theta[°] | d [Å] | I/10 (peak height) | Counts (peak area) | FWHM | Hklvalue | Size (nm) | Phase Name | JCPDS File NO. |
|-----------|--------|--------------------------|--------------------------|--------|----------|-----------|------------|-------------------|
| 10.85 | 8.1460 | 107.59 | 17.64 | 1.3345 | 1 1 0 | 6.255584 | Hornblende | 87-0611 |
| 12.12 | 7.2977 | 68.27 | 15.72 | 1.8734 | 1 0 0 | 4.451147 | Microcline | 87-1792 |
| 13.84 | 6.3952 | 74.03 | 11.84 | 1.3018 | 0 2 0 | 6.394647 | Microcline | 87-1792 |
| 17.66 | 5.0170 | 180.46 | 5.35 | 0.2411 | 0 0 2 | 34.36853 | Olivine | 85-1682 |
| 19.26 | 4.6044 | 19.25 | 0.57 | 0.2411 | 1 3 0 | 34.29064 | Hornblende | 87-0611 |
| 20.29 | 4.3740 | 61.03 | 1.81 | 0.2411 | 1 1 0 | 34.23696 | Biotite | 88-2200 |
| 20.53 | 4.3232 | 13.74 | 0.41 | 0.2411 | 0 3 0 | 34.22405 | Microcline | 87-1792 |
| 21.25 | 4.1776 | 57.41 | 1.70 | 0.2411 | 0 2 1 | 34.18443 | Biotite | 88-2200 |
| 21.88 | 4.0582 | 47.70 | 1.41 | 0.2411 | 2 0 1 | 34.14866 | Hornblende | 87-0611 |
| 22.61 | 3.9300 | 18.36 | 0.54 | 0.2411 | 1 1 0 | 34.10592 | Microcline | 87-1792 |
| 23.00 | 3.8639 | 23.72 | 0.70 | 0.2411 | 2 1 1 | 34.08251 | Microcline | 87-1792 |
| 23.84 | 3.7290 | 112.08 | 3.32 | 0.2411 | 1 1 1 | 34.03077 | Microcline | 87-1792 |
| 24.51 | 3.6296 | 107.15 | 3.17 | 0.2411 | 1 3 0 | 33.98818 | Microcline | 87-1792 |
| 24.90 | 3.5733 | 207.44 | 6.15 | 0.2411 | 1 3 1 | 33.96286 | Microcline | 87-1792 |
| 25.95 | 3.4304 | 393.59 | 11.66 | 0.2411 | 2 1 0 | 33.89273 | Microcline | 87-1792 |
| 26.92 | 3.3097 | 214.75 | 12.73 | 0.4822 | 1 2 1 | 16.91271 | Microcline | 87-1792 |
| 28.09 | 3.1738 | 824.27 | 24.42 | 0.2411 | 2 0 2 | 33.74099 | Microcline | 87-1792 |
| 29.27 | 3.0489 | 49.85 | 2.22 | 0.3617 | 2 1 2 | 22.43176 | Microcline | 87-1792 |
| 29.99 | 2.9770 | 70.19 | 3.64 | 0.4220 | 1 2 2 | 19.19454 | Microcline | 87-1792 |
| 30.74 | 2.9058 | 67.94 | 11.57 | 1.3864 | 1 4 1 | 5.83217 | Microcline | 87-1792 |
| 31.77 | 2.8143 | 17.87 | 1.06 | 0.4822 | 0 2 2 | 16.72629 | Microcline | 87-1792 |
| 32.61 | 2.7434 | 30.26 | 0.90 | 0.2411 | 1 8 2 | 33.38189 | Microcline | 87-1792 |
| 33.07 | 2.7069 | 13.76 | 0.51 | 0.3014 | 0 2 3 | 26.67173 | Biotite | 88-2200 |
| 34.06 | 2.6301 | 36.59 | 1.63 | 0.3617 | 1 1 2 | 22.16738 | Hornblende | 87-0611 |
| 35.78 | 2.5077 | 60.72 | 6.30 | 0.8439 | 2 0 2 | 9.456306 | Biotite | 88-2200 |
| 37.04 | 2.4248 | 62.43 | 2.31 | 0.3014 | 4 0 1 | 26.38145 | Hornblende | 87-0611 |
| 38.16 | 2.3565 | 60.79 | 2.25 | 0.3014 | 1 4 2 | 26.29382 | Microcline | 87-1792 |
| 39.91 | 2.2572 | 95.43 | 3.53 | 0.3014 | 1 1 3 | 26.15187 | Microcline | 87-1792 |
| 40.27 | 2.2377 | 49.48 | 5.86 | 0.9645 | 3 3 1 | 8.162927 | Microcline | 87-1792 |
| 41.05 | 2.1968 | 34.86 | 1.81 | 0.4220 | 2 5 1 | 18.60974 | Microcline | 87-1792 |
| 41.87 | 2.1560 | 67.61 | 9.01 | 1.0850 | 3 3 2 | 7.2185 | Microcline | 87-1792 |
| 42.83 | 2.1096 | 300.12 | 11.12 | 0.3014 | 3 0 3 | 25.90145 | Microcline | 87-1792 |
| 44.10 | 2.0520 | 80.84 | 3.59 | 0.3617 | 1 3 2 | 21.48821 | Olivine | 85-1682 |
| 44.52 | 2.0335 | 54.51 | 2.02 | 0.3014 | 1 6 0 | 25.74882 | Microcline | 88-2376 |

| | | | | | | | | |
|-------|--------|--------|-------|--------|--------|----------|-------------|---------|
| 45.84 | 1.9777 | 236.46 | 8.76 | 0.3014 | 3 7 1 | 25.62571 | Hornblende | 87-0611 |
| 46.24 | 1.9619 | 85.72 | 9.52 | 0.9042 | 2 0 2 | 8.529243 | Microcline | 87-1792 |
| 47.19 | 1.9310 | 48.52 | 6.11 | 1.0248 | 6 1 2 | 7.498614 | Hypersthene | 76-0490 |
| 48.20 | 1.8866 | 77.35 | 2.86 | 0.3014 | 8 2 1 | 25.39714 | Biotite | 88-2200 |
| 49.31 | 1.8465 | 126.36 | 5.62 | 0.3617 | 4 0 3 | 21.07042 | Microcline | 87-1792 |
| 50.52 | 1.8052 | 146.18 | 4.33 | 0.2411 | 3 3 1 | 31.45504 | Microcline | 87-1792 |
| 51.12 | 1.7853 | 331.59 | 10.26 | 0.2517 | 3 4 3 | 30.0555 | Microcline | 87-1792 |
| 51.93 | 1.7593 | 31.82 | 4.25 | 1.0867 | 0 6 2 | 6.937707 | Microcline | 87-1792 |
| 52.72 | 1.7349 | 34.19 | 6.23 | 1.4828 | 1 1 5 | 5.067249 | Biotite | 88-2200 |
| 53.59 | 1.7087 | 47.97 | 2.88 | 0.4893 | 0 6 0 | 15.29784 | Olivine | 85-1682 |
| 54.19 | 1.6911 | 55.02 | 1.23 | 0.1816 | 1 5 1 | 41.10868 | Olivine | 85-1682 |
| 54.86 | 1.6722 | 30.75 | 0.70 | 0.1848 | 1 3 5 | 40.27531 | Olivine | 85-1682 |
| 55.31 | 1.6596 | 29.21 | 0.35 | 0.0965 | 0 6 1 | 76.97047 | Olivine | 85-1682 |
| 55.76 | 1.6472 | 54.62 | 1.62 | 0.2411 | 2 3 2 | 30.74371 | Hypersthene | 76-0490 |
| 57.06 | 1.6128 | 24.38 | 0.72 | 0.2411 | 1 5 1 | 30.55722 | Biotite | 88-2200 |
| 57.66 | 1.5974 | 21.23 | 0.47 | 0.1808 | 1 1 3 | 40.63205 | Hornblende | 87-0611 |
| 59.41 | 1.5545 | 28.14 | 0.63 | 0.1808 | 1 5 3 | 40.28577 | Hornblende | 87-0611 |
| 59.89 | 1.5431 | 16.48 | 0.37 | 0.1808 | 3 0 1 | 40.18914 | Olivine | 85-1682 |
| 60.58 | 1.5271 | 64.18 | 2.38 | 0.3014 | 3 1 1 | 24.02409 | Olivine | 85-1682 |
| 62.57 | 1.4833 | 60.50 | 2.24 | 0.3014 | 2 0 3 | 23.77679 | Hornblende | 87-0611 |
| 63.39 | 1.4662 | 31.85 | 1.65 | 0.4220 | 2 10 2 | 16.90753 | Hornblende | 87-0611 |
| 64.59 | 1.4417 | 61.54 | 2.74 | 0.3617 | 3 3 0 | 19.5976 | Olivine | 85-1682 |
| 64.86 | 1.4363 | 33.49 | 2.48 | 0.6028 | 6 6 1 | 11.74166 | Hornblende | 87-0611 |
| 65.59 | 1.4222 | 20.16 | 0.60 | 0.2411 | 1 1 4 | 29.23718 | Olivine | 85-1682 |
| 66.10 | 1.4124 | 36.83 | 1.09 | 0.2411 | 6 0 1 | 29.15305 | Hornblende | 87-0611 |
| 67.09 | 1.3939 | 63.52 | 1.88 | 0.2411 | 2 5 3 | 28.98809 | Olivine | 85-1682 |
| 68.39 | 1.3706 | 107.12 | 7.14 | 0.5425 | 7 3 1 | 12.78527 | Hornblende | 87-0611 |
| 68.90 | 1.3616 | 363.83 | 13.48 | 0.3014 | 1 7 3 | 22.94282 | Hornblende | 87-0611 |
| 69.72 | 1.3477 | 28.18 | 1.25 | 0.3617 | 6 4 1 | 19.02362 | Hornblende | 87-0611 |
| 70.14 | 1.3406 | 38.58 | 1.43 | 0.3014 | 8 5 1 | 22.77117 | Hypersthene | 76-0490 |
| 72.64 | 1.3005 | 28.35 | 0.63 | 0.1808 | 0 6 3 | 37.36997 | Olivine | 85-1682 |
| 74.24 | 1.2764 | 19.98 | 0.59 | 0.2411 | 1 7 2 | 27.73324 | Olivine | 85-1682 |
| 75.62 | 1.2564 | 57.10 | 2.11 | 0.3014 | 1 4 4 | 21.98095 | Olivine | 85-1682 |
| 75.62 | 1.2564 | 57.10 | 2.11 | 0.3014 | 1 4 4 | 21.98095 | Olivine | 85-1682 |
| 76.68 | 1.2418 | 46.96 | 1.74 | 0.3014 | 3 1 3 | 21.82223 | Olivine | 85-1682 |
| 78.09 | 1.2227 | 51.50 | 2.67 | 0.4220 | 1 8 1 | 15.43298 | Olivine | 85-1682 |
| 78.49 | 1.2176 | 40.57 | 1.20 | 0.2411 | 3 2 3 | 26.93588 | Olivine | 85-1682 |
| 80.02 | 1.1981 | 39.83 | 1.18 | 0.2411 | 4 0 0 | 26.6397 | Olivine | 85-1682 |

3.5. Microstructures

Rock samples from the study area were applied to examine the microstructure. Based on the images obtained from the petrographic microscope images combined with the Scanning Electron Microscope (SEM).

3.5.1. Dolerite

The observed microstructures (Fig. 7) are in three types; micro cracks–intra-granular, intergranular and transgranular. The micro-cracks are seen through SEM images showing alternating wedges of the augite and labradorite grain boundary (Olivine). Curved ends of two augite wedges are encircled (white dashed line). The impact generated microfractures in the augite wedge cease in the adjacent labradorite wedges. The grains adjacent to the augite and labradorite do not have wedges is similar to cases where multiple PF sets are produced in a particular grain, while the surrounding grains are left undeformed [19, 20, 21]. The microfractures were filled possibly with the labradorite from the adjacent wedge. The bulk labradorite contains sharp spots and diffused background. The labradorite in bulk crystal demonstrated perfectly aligned, well-developed lattice planes and the absence of amorphous components. The granite's compositional variability, which represents the rapid termination of the anatectic processes and the modification of the P-T conditions, is related to a shift from a compressional to an extensional tectonic setting extension regime [22].

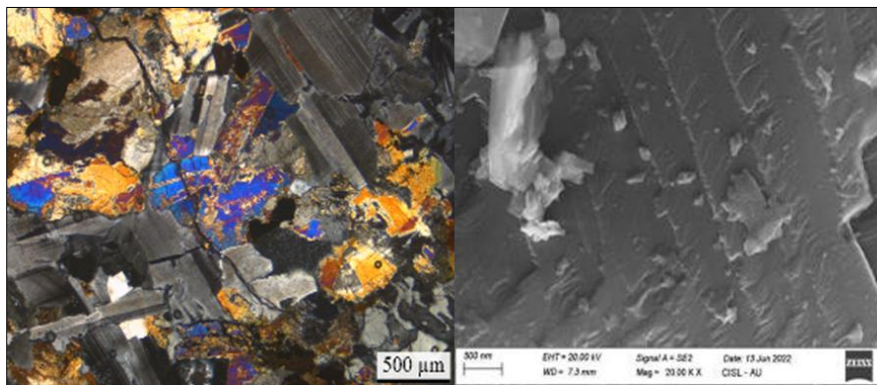


Figure 7 Microstructures of dolerite rock.

Compositionally, dolerite is characterized by a combination of quartz, augite, and plagioclase feldspar [23]. In order to confirm the form of $[\text{SiO}_2\text{-NaAlSi}_3\text{O}_8\text{-Al}_2\text{Si}_2\text{O}_8\text{-(Ca, Na) (Fe, Mg, Al-Ti) (Si, Al}_2\text{O}_6)]$ EDAX analysis was performed. During EDAX measurement, different areas were focused and the corresponding peaks (Figure 8). The chemical composition elements can be seen in sample No.1 in the EDAX peak spectrum. In peak spectrum, the quantity of carbon 18.35%, oxygen 65.31%, sodium 0.95%, Aluminium 0.50%, silica 7.34%, calcium 1.96%, chromium 0.08%, promethium 0.1% is measured in atomic weight respectively. In the given data, the oxygen percentage is higher when compared to other elements followed by silica. So, in this case, quartz (SiO_2) is rich in the given rock sample. Promethium is a chemical element with the symbol Pm. Its isotopes are radioactive element which is present in the specimen. The dolerite elemental percentage detected from FESEM-EDAX is shown in Table 3.

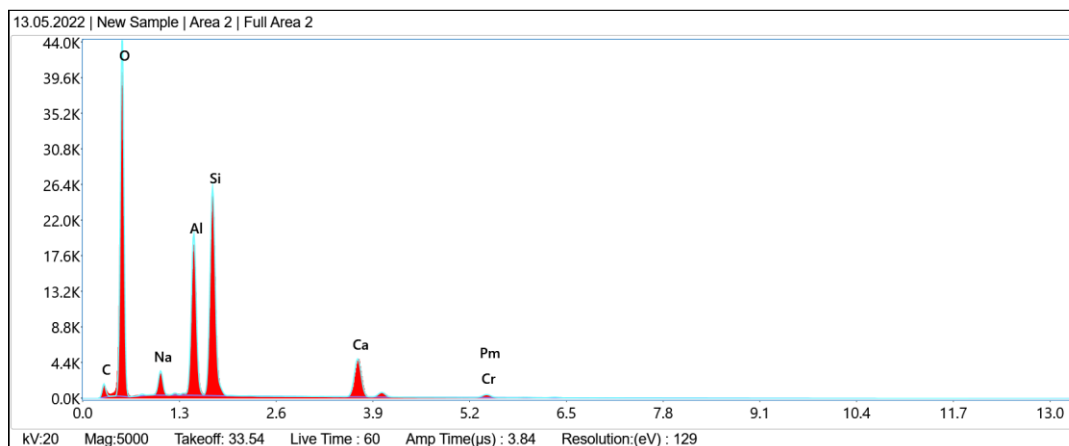


Figure 8 EDAX measurement dolerite.

Table 3 The dolerite elemental percentage detected from FESEM-EDAX

| Element | Weight% | MDL | Atomic% | Error% | Net Int. | R | A | F |
|---------|---------|------|---------|--------|----------|--------|--------|--------|
| CK | 12.58 | 0.3 | 18.35 | 12.06 | 133.17 | 0.9113 | 0.0542 | 1.0000 |
| OK | 59.65 | 0.07 | 65.31 | 9.62 | 4391.71 | 0.9215 | 0.1475 | 1.0000 |
| NaK | 1.25 | 0.11 | 0.95 | 10.99 | 157.67 | 0.9330 | 0.2369 | 1.0043 |
| AlK | 9.08 | 0.03 | 5.90 | 6.24 | 2628.03 | 0.9397 | 0.5035 | 1.0081 |
| SiK | 11.76 | 0.02 | 7.34 | 5.65 | 3576.23 | 0.9428 | 0.5571 | 1.0043 |
| CaK | 4.49 | 0.04 | 1.96 | 2.83 | 882.04 | 0.9586 | 0.9032 | 1.0204 |
| CrK | 0.24 | 0.09 | 0.08 | 12.26 | 32.60 | 0.9674 | 0.9602 | 1.0551 |
| PmL | 0.95 | 0.21 | 0.11 | 18.46 | 48.84 | 0.9703 | 0.9664 | 1.0134 |

3.5.2. Charnockite

The charnockite collected from the Yellikkaradu study area was studied under petrographic and SEM. The image (Figure 9) displaces an interconnection of two sets of perpendicular micro-cracks in the pyroxene grain; because they are the cleavage micro cracks. These micro-cracks show a constant pattern forming a circular area around a small area of a homogeneous microstructure. In the thin section image, there is a presence of the interpenetration of grain boundaries.

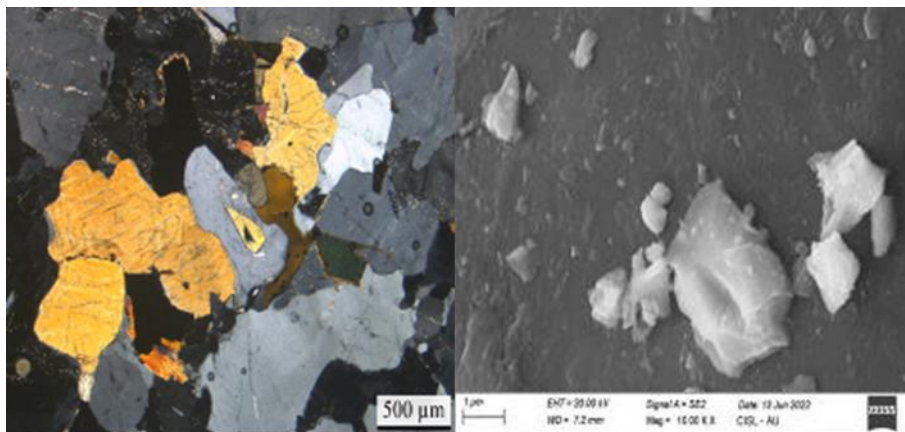


Figure 9 Microstructures of charnockite rock.

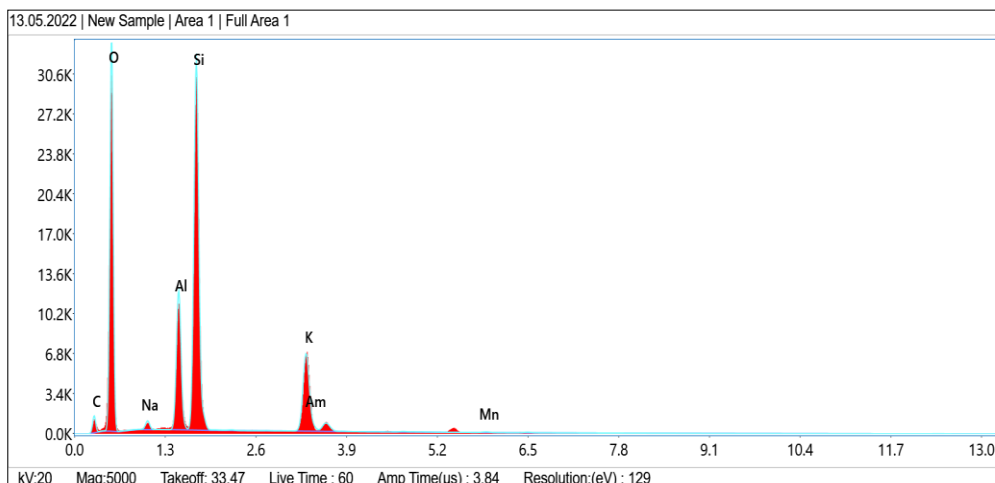


Figure 10 EDAX measurement peaks of charnockite rock.

Table 4 The charnockite elemental percentage detected from FESEM-EDAX

| Element | Weight% | MDL | Atomic% | Error% | Net Int | R | A | F |
|---------|---------|------|---------|--------|---------|--------|--------|--------|
| CK | 13.35 | 0.3 | 19.68 | 12.10 | 118.10 | 0.9095 | 0.0528 | 1.0000 |
| OK | 56.80 | 0.07 | 62.86 | 9.78 | 3310.95 | 0.9197 | 0.1360 | 1.0000 |
| NaK | 0.75 | 0.06 | 0.58 | 11.96 | 82.40 | 0.9314 | 0.2397 | 1.0040 |
| AlK | 6.14 | 0.03 | 4.03 | 6.23 | 1566.90 | 0.9383 | 0.5167 | 1.0097 |
| SiK | 15.85 | 0.03 | 9.99 | 5.31 | 4384.72 | 0.9414 | 0.5901 | 1.0046 |
| KK | 6.11 | 0.04 | 2.77 | 3.03 | 1181.44 | 0.9551 | 0.8673 | 1.0144 |
| MnK | 0.12 | 0.07 | 0.04 | 25.58 | 11.46 | 0.9687 | 0.9656 | 1.0663 |
| AmM | 0.89 | 0.2 | 0.06 | 13.87 | 66.41 | 0.9578 | 0.8760 | 1.0058 |

Compositionally, charnockite is characterized by a combination of quartz, hypersthene, microcline, hornblende, olivine, and biotite. To confirm the form of $[\text{SiO}_2\text{-KAlSi}_3\text{O}_8\text{-(Ca, Na)}_2\text{ (Mg, Fe, Al)}_5\text{ (Al, Si)}_8\text{ MgFe}^{2+}\text{(Mg, Fe) (Al, Si)O (F, OH)}]$ EDAX analysis was performed. During EDAX measurement different areas were focused and the corresponding peaks were shown in Figure 10. The chemical composition elements can be seen in the sample in the EDAX peak spectrum. In the peak spectrum, the quantity of carbon 19.68%, oxygen 62.86%, sodium 0.58%, aluminium 4.03%, silica 9.99%, calcium 2.77%, potassium 2.77%, manganese 0.04%, americium 0.06% is measured in atomic weight respectively. In the given data the peak value of Si and O is higher. So, in this case, quartz (SiO_2) is rich in the given rock sample. Manganese is present in this rock. Americium is a chemical element with the symbol Am. It is an isotope radioactive element present in the specimen. The charnockite elemental percentage detected from FESEM-EDAX is shown in Table 4.

4. Conclusion

Both the samples (dolerite and charnockite) exhibit a sub-ophitic texture based on petrographic analysis, and the mineral assemblages of the XRD measurement reveal that plagioclase feldspar, augite, and quartz as an essential minerals. The intergrowth granophyric texture firmly demonstrates the intrusion of the youngest magma with older rock. The oldest Archean granulitic rocks were formed in that terrain with structural disturbances such as faults, joints, etc.,. Later, due to late magmatism, the lava is emplaced in that structures. The mineral percentage of quartz is rich in the rocks because of intergrowth texture and the cooling temperature and pressure of the rocks are low so the magma crystallized rapidly above the surface. Hence, the crystallizing temperature of the quartz is low. Thus, the rocks contain a significant proportion of quartz. Thus, it is a quartz-dolerite rock.

Compliance with ethical standards

Acknowledgments

The authors are thankful to Mr. V.M. Sakthivel, Divisional Manager, TAMIN for his permission and valuable support to carry out this research work. The authors would like to acknowledge the Centralized Instrumentation and Service Laboratory (CISL), Annamalai University for facilitating the instruments to carry out SEM analysis.

Disclosure of conflict of interest

We don't have any conflict of interest in publishing the paper.

References

- [1] Armstrong R.L. and Besanon J. A Triassic time scale dilemma, K-Ar dating of upper Triassic mafic igneous rocks of eastern U.S.A and Canada and post upper Triassic plutons, Western Idaho, U.S.A *Eclogae Geol. Helv.* 1970; (63):15-38.
- [2] Boer J.de. Paleomagnetic-tectonic study of Mesozoic dyke swarms in the Appalachians *J. Geophys. Res.* 1967; (72):2237-2250.

- [3] Bryan S. E. and Ernst R. E. Revised definition of Large Igneous Provinces (LIPs). *Earth Sci. Rev.* 2008; (86):175-202.
- [4] Rao V.D., Rao P.R. and Rao M. S. The Ghingee Granite, Tamil Nadu, South India. *Geochemistry and Petrogenesis. Gondwana Research.* 1999; (1):117-26.
- [5] Don Herms O. L. A quantitative petrographic study of Dolerite in the deep river basin of North Carolina. *Journal of Earth and Planetary Materials.* 1964; (11-12):1718-29.
- [6] Ernst R.E and Buchan K.L. Large mafic magmatic events through time and links to mantle-plume heads. *Mantle Plumes their identification through Time. Geological Society of America* (2001); 352, 483–575.
- [7] Foley S.F., Venturelli G., Green D.H., and Toscani L. The ultra potassic rocks characteristics, classification, and constraints for petrogenetic models. *Earth-Science Reviews.* 1987; (24):81–134.
- [8] French B. M., Kocberl C., Gilmour I., Shiery S. B., Dons J.A., and Naterstad J. The Gardnos impact structure, Norway. *Petrology and geochemistry of target rocks and impactites. Geochemica et Cosmochimica Acta.*1997; Issue 4, p. 873-904. DOI: 10.1016/S0016-7037(96)00382-1
- [9] French B. M., Cordua W. S., and Plescia J. B. The rock El meteorite impact structure, Wisconsin: Geology and shock-metamorphic effects in quartz. *Geological Society of America Bulletin.* 2004; 116(1-2):200-218.
- [10] Halls H.C. The importance and potential of mafic dyke swarms in studies of geodynamic processes. *Geoscience Canada.* 1982; (9):145–154.
- [11] Hou G.T., Santosh M., Qian X.L., Lister G.S. and Li J.H. Configuration of the Late Paleoproterozoic supercontinent Columbia. Insights from radiating mafic dyke swarms. *Gondwana Research.* (2008); (14):395–409. DOI:10.1016/j. gr.2008.01.010.
- [12] Justus, P.S. Modal and textural zonation of diabase dykes, Deep River Basin, North Carolina. [M.Sc. Dissertation]. University of North Carolina; 1966.
- [13] Kieffer. Shock metamorphism of the Coconino sandstone at meteor crater, Arizona. *Journal of Geophysical research.* 1971; (76):5449-473.
- [14] King, P.B. Systematic pattern Survey of Triassic dykes in the Appalachian region. *U. S. Geol. Professional papers.* 1961; 424-B, B93-B95.
- [15] Lawrence, D.E. A contribution to the petrology of the Great Dyke of Nova-Scotia. M.Sc. Thesis, Dalhousie University, 108 p. (1966).
- [16] Le Cheminant A.N, and Heaman L.M. Mackenzie. Igneous events, Canada Middle Proterozoic hotspot magmatism associated with ocean opening. *Earth Planet. Sci. Lett.* 1989; (96):38-48.
- [17] Liu S., Zou H.B., Hu R.Z., Zhao J.H. and Feng C. X. Mesozoic mafic dykes from the Shandong Peninsula, North China Craton. *Petrogenesis and tectonic implications. Geochemical Journal.* 2006; (40):181–195. DOI:10.2343/ geochem J.40.181.
- [18] Marsh J.S. Geochemical constraints on compiled assimilation and fractional crystallization involving upper crustal compositions and continental theolitic magma. *Earth planet. Sci. Lett.* 1989; 92,70-80.
- [19] Mathew Joseph. *Geochemistry, petrogenesis and palaeomagnetism of the dyke swarms of Thiruvannamalai area, Tamil Nadu and the lithospheric processes-in South India.* Seymour K.S and Kumaraplli, P.S (1995) *Geochemistry of the Grenville dyke swarm: role of plume-source mantle in magma genesis.* *Contrib Mineral., petrol.,* 120,29-41.
- [20] Shrivastava V. S. X-ray Diffraction and Mineralogical Study Soil. A Review. *J Appl. Chem. Res.* 2009; (9): 41–51.
- [21] Steele, K. F, Ragland P.C. Model for the closed system Fractionation of a Dyke formed by two pulses of Dolerite Magma. *Contributions to Mineralogy and Petrology.* 1976; 57(3):305-316.
- [22] Steffer D and Langerhorst F. Shock metamorphism of quartz in nature and experimental. *Basic observation and theory meteorites.* 1994; (2):115-181.
- [23] Zhao J.X., and McCulloch M.T. Melting of a subduction-modified continental lithospheric mantle. Evidence from Late Proterozoic mafic dyke swarms in central Australia: *Geology.* 1993; (21):463–466.